ELSEVIER

PII: S0032-3861(97)00465-5

*Polymer* Vol. 39 No. 10, pp. 1765–1778, 1998

0032-3861/98/$19.00+0.00

# Effects of morphology on the toughness of styrene–butadiene–styrene triblock copolymer/ methyl methacrylate–styrene copolymer blends

**Ikuro Yamaoka**
*New Materials Division, Nippon Steel Corporation, 6-3, Otemachi 2-chome, Chiyoda-ku, Tokyo 100-71, Japan*
*(Received 18 December 1996; revised 21 May 1997)*

Poly(styrene-*block*-butadiene-*block*-styrene) triblock copolymer (KR05) was melt mixed with methyl methacrylate–styrene copolymer (MS-200) in an internal mixer, and the resultant blends were compression moulded to examine the morphology and the mechanical properties. KR05 in KR05/MS-200 blends incorporated in an internal mixer exhibits an alternate lamellar structure between the PB and the PS phases, and phase separation from MS-200 as reported previously for the twin-screw extruded blends. Internal mixing should be a powerful tool for melt mixing of KR05 with MS-200, since KR05/MS-200 blends after internal mixing could roughly parallel those after partially intermeshing counter-rotating twin-screw extrusion in degree of mixing. Ductile KR05 is toughened by incorporation of brittle MS-200 and synergistic improvement of the impact strength is observed for compression mouldings of the blends with the composition between 10 and 30 wt% MS-200. When the composition of KR05/MS-200 blends was varied, MS-200 domain morphology appropriate for toughening the blends was examined. In this case KR05/MS-200 blends are remarkably toughened with the morphology that spherical MS-200 domains ranging from 0.3 to 0.5 $\mu$m in actual diameter are densely dispersed in orderly lamellae of the KR05 matrix. 

**(Keywords: internal mixer; impact strength; domain size analysis)**

## INTRODUCTION

Enhancing the toughness of polymers is of great importance for their practical use. One of the well-known toughening techniques in industrial polymer processing is based on biaxial orientation of polymer chains. This is a simple and useful, but applicable only when polymers are processed through biaxial stretching into films, sheets, bottles or their analogues. Polymer alloying is put to industrial use for improving various kinds of properties of polymers, and needless to say, this is one of the toughening techniques of polymers. It should be stressed that this has good applicability to toughening of a wide variety of polymeric products, in contrast to the limited applicability of biaxial stretching.

It is conventionally recognized that polymers are often alloyed with polymeric impact modifiers in order for the resultant polymer alloys to have the microdomain morphology responsible for their effective toughness enhancement. In such cases rubber toughening must be the most typical and widespread methodology, but it should be noted that among toughened polymer alloys, some are toughened with mechanism in striking contrast to rubber toughening. These alloys of interest possess brittle inclusions incorporated into the ductile polymeric matrix[1–9]. Commercial polymer blends composed of poly(styrene-*block*-butadiene-*block*-styrene) triblock copolymer (KR05, Phillips Petroleum Co.) with methyl methacrylate–styrene copolymer (MS-200, Nippon Steel Chemical Co.) are classified into this category[7–9]. The toughness of KR05-enriched KR05/MS-200 blends is doubled or enhanced more depending on their composition and morphology, compared with that of neat KR05. This effective toughening enhancement is attained only by using the simplest alloying technique, that is to say, nonreactive melt blending on which no chemical linkage between the two component polymers results. Prominent synergistic improvement in their impact strength is obtained when the ductile KR05 phase, which exhibits alternate lamellar type separation between the polystyrene (PS) and the polybutadiene (PB) phases, is ordered and the brittle MS-200 domains suspended in the KR05 phase are spherical[8]. On impact to the KR05-enriched KR05/MS-200 blends, effective energy dissipation results from shear yielding of the KR05 matrices, microcavitation in the PB lamellae and debonding in the KR05/MS-200 interfacial regions[7,8]. In this study, the previous investigation of structure–impact property relationships of KR05/MS-200 blends has been further developed, and MS-200 domain morphology appropriate for toughening the blends has been examined.

It is well known that twin-screw extrusion is extensively used for melt blending of polymers to give desirable degree of mixing. However, the twin-screw extruder which the author used previously for mixing KR05 with MS-200, hereafter referred to as the 'Lab-extruder', brought no good dispersion of MS-200 domains in the KR05 matrix[7–9]. The following three reasons account for the poor and uneven dispersion produced through the Lab-extruder.

(1) Full-flighted screws of the Lab-extruder were not equipped with any mixing sections, and consequently, could not give the polymer melt high enough shear and effective enough distributive mixing enough to attain desirable degree of mixing of KR05/MS-200 blends.

When the Lab-extruder (partially intermeshing twin-screw extruder) and the corresponding non-intermeshing twin-screw extruder have screws with the same geometrical design, their melt conveying characteristics must be analogous to each other, because of their similarity in spatial configuration between the two screws in the barrel. Therefore, their mixing performance would be analogous although melt flow in the nip region is somewhat different between the two extruders. Since the melt conveying of the latter extruder is also similar to that of a single-screw extruder when they have the same screw geometry[10,11], the melt conveying property of the Lab-extruder can be roughly estimated by considering that of a single-screw extruder with the corresponding screw geometry. Equipping the single-screw extruder with only one distributive mixing section could result in no less than three orders of magnitude improvement of degree of mixing when the extruder imposes a strain of $10^4$ on the melt being mixed[12–15]. Accordingly, the Lab-extruder also could have produced much better domain dispersion if it had been equipped with at least one mixing section.

(2) Average residence time of the melt on the full-flighted screws of the Lab-extruder was definitely short since they had no mixing sections which could valve the melt flow along the screw axes. The short residence time was also responsible for its poor mixing performance.

(3) The Lab-extruder was a partially intermeshing extruder with a system open in the axial direction of the screws from the inlet to the outlet of the extruder barrel, in which the melt on mixing was easily pushed backward along the screw axes due to backpressure[16,17]. Consequent on such backflow, the melt was subject to very broad residence time distribution in the barrel[18], although the average residence time was short as mentioned above. This could lead to uneven dispersion of MS-200 domains, which ranges from submicrometres to more than 10 micrometres in size. In order to attain a suitable degree of mixing two-fold extrusion had to be done.

Here the use of the above-mentioned extruder was given up, and instead a laboratory internal mixer was tried for melt blending of KR05 and MS-200. An internal mixer has a pair of counter-rotating, non-intermeshing winged rotors parallelled in a closed chamber, which has a gourd-shaped cross section perpendicular to the rotor axes. The rotors are mostly geared to have different rotational speeds[19–23]. Internal mixers have been used widely for polymer blending and compounding, and rubber kneading both in industry and on laboratory scales, because of their mechanical simplicity and good mixing performance. Since wings on their rotating rotors produce intensive laminar shear mixing in the circumferential direction of the rotors, and effective distributive mixing in the axial direction[24], it was expected to bring desirable degree of mixing and even fine dispersion of MS-200 domains in the KR05 matrix. However, it should be stressed that the principal reason why the author employed an internal mixer here is that it has great advantage over screw extruders concerning residence time control of the polymer melt being mixed. Any residence time of the polymer melt in the mixer chamber can be set with no residence time distribution, independent of the other processing conditions. Flow in internal mixers was observed[20,21,25–27] and simulated[22,28–31] well with various processing conditions, which was of help to determine the mixing condition for KR05 and MS-200.

## EXPERIMENTAL

### *Materials*

The commercial star-shaped poly(styrene-*block*-butadiene-*block*-styrene) triblock copolymer (SBS) and the commercial methyl methacrylate–styrene copolymer (MS) used here are the same polymers as chosen in the author's previous studies[7–9,32]. The star-shaped SBS, which is prepared by two-stage sequential addition of styrene and butadiene monomers for an anionic polymerization and by coupling the resultant living ends[33,34], is supplied by Phillips Petroleum Company under the tradename of K-Resin KR05. The number- and weight-average molecular weights ($M_n$ and $M_W$) and their polydispersity coefficient ($M_W/M_n$) for KR05 used, measured by gel permeation chromatography (g.p.c.), are $5.23 \times 10^4$, $1.51 \times 10^5$ and 2.89, respectively. Nuclear magnetic resonance (n.m.r.) measurements revealed that the weight fraction ($\phi_w$) of a PS block component for KR05 is 0.755. Measurements by differential scanning calorimetry (d.s.c.) showed two distinct glass transitions ($T_g$s), near −80°C and 95°C, corresponding to the PB phase and the PS phase, respectively. The KR05 was melt mixed with the MS supplied by Nippon Steel Chemical Company under the tradename of MS-200. $M_n$, $M_W$ and $M_W/M_n$ for the MS-200 used, measured by g.p.c., are $1.00 \times 10^5$, $2.30 \times 10^5$ and 2.30, respectively. The $\phi_w$ of a styrene component for MS-200 is 0.78. The polymers were used as received, and neither chemical nor physical modification was done before melt processing.

### *Sample preparation*

*Melt mixing.* MS-200 was dried in an oven at 80°C for 4 h and was dry-blended with different weight ratios of KR05, specifically being −90, 85, 80, 75, 70, 50, and 25 wt% KR05. Melt mixing was carried out in a laboratory scale internal mixer of Toyo Seiki Seisaku-sho, Ltd., with triple winged rotors recommended for high shear applications, which have a close geometrical analogy with many internal mixers in industrial and laboratorial use. The two rotors were geared at the rotational speed ratio of 3/2 as usually set for practical internal mixers used to blend polymers. Hereafter melt mixing in an internal mixer is termed 'internal mixing' as found in much literature[35,36], and the resultant blends are referred to as 'internally-mixed' blends. For kneading of a neat polymer in an internal mixer the term 'internally-kneaded' is employed.

*Mixing conditions.* Preliminary examination was done in order to determine mixing conditions suitable to attain appropriate degree of mixing and uniform distribution of MS-200 domains in the KR05 matrix without appreciable thermal degradation of the polymers. The chamber temperature of the mixer was set at 180°C, which is 20–40°C lower than the temperature for kneading of common styrenic polymers, in order to avoid unnecessary thermal degradation of the PB block of KR05 for long mixing (10 min, see below). Note that most of the melt mixers available on industrial or laboratorial scales (extruders, internal mixers, mixing rolls, etc.) are not run effectively for styrenic polymers at temperatures below 180°C, because of the greatly enhanced motor torque consequent on the very high melt viscosity of the polymers.

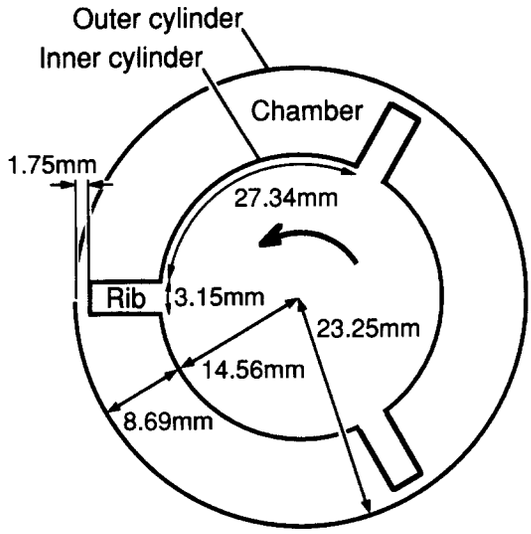


**Figure 1** Schematic view of a simple internal mixer made of two concentric cylinders. Sizes shown in the geometry were calculated for the internal mixer used here

The effective shear rate $\dot{\gamma}_{eff}$ in triple winged internal mixers can be estimated by using a model of a simplified internal mixer[19,23,37]. *Figure 1* shows the model for the mixer used here. This model is composed of a mixing chamber, which is made of the space between concentric outer and inner cylinders of infinite length, and three ribs, which are projected at identical intervals from the inner cylinder in the chamber. The tops of the ribs make three narrow gaps to the outer cylinder wall. Three ribs and three deep sections alternate along the circumference of the inner cylinder in the chamber, being modelled after the arrangement of three wings on the rotor in practical internal mixers. $\dot{\gamma}_{eff}$ can be calculated on the simplifying assumptions of laminar, isothermal steady and incompressible Newtonian flow in the chamber, no slip of the polymer melt at the walls, negligible entrance and exit effects of the melt around the narrow gaps, and neglecting the gravitational force. When mixing is done in the internal mixer used here at rotational speeds of $N$ r.p.m. and $(2/3)N$ r.p.m. for respective rotors, the $\dot{\gamma}_{eff}$ range is estimated for the geometry of the corresponding simplified model as

$$0.187N\ s^{-1}(\dot{\gamma}_{eff,min}) \leq \dot{\gamma}_{eff} \leq 2.49N\ s^{-1}(\dot{\gamma}_{eff,\ max}) \quad (1)$$

$\dot{\gamma}_{eff,\ min}$ here is the shear rate for pure drag flow in the deep section on the lower speed rotor, and $\dot{\gamma}_{eff,max}$ the maximum shear rate at the chamber wall in gaps between wing tips of the higher speed rotor and the wall. Increasing rotational speed was considered to be better for enhancing degree of mixing. However, when rotational speeds of the higher speed rotor were set over 70 r.p.m. ($\dot{\gamma}_{eff,max} > 174\ s^{-1}$), the monitored motor torque of the mixer scarcely increased as rotational speed increased and thermal degradation of the PB block was found to be accelerated at any chamber temperatures examined preliminarily (160–240°C). These could be due to large temperature increase of the polymer melt resulting from harsh shear produced at the narrow gaps. Accordingly, the rotational speed of 70 r.p.m. was employed for the higher speed rotor here, and therefore, the $\dot{\gamma}_{eff}$ range under the mixing condition employed here is given as

$$13.1\ s^{-1} \leq \dot{\gamma}_{eff} \leq 174\ s^{-1} \quad (2)$$

Of the chamber capacity, 70–80 vol% was filled with materials, to attain the most effective distributive mixing[19]. A long residence time of 10 min was employed to avoid uneven mixing. This is the longest permissible mixing time for KR05/MS-200 blends in the internal mixer, since it took at most 10 min to level off the monitored motor torque on mixing, and mixing over 10 min often brought perceivable thermal degradation of the PB block.

Just after completion of mixing, lumps of the hot melt were taken out of the mixer quickly, made into disks irregular in shape (4–5 cm in diameter, less than 1 cm in thickness) and cooled rapidly in water.

The compositions of the blends are indicated as weight percentages, KR05/MS-200. For example, KR05/MS-200(85/15) represents a blend of 85 wt% KR05 and 15 wt% MS-200.

Comparison of the $\dot{\gamma}_{eff}$ level produced on melt mixing between the internal mixer used here and the Lab-extruder used previously may verify the superiority in the mixing performance of the former. The assessment of $\dot{\gamma}_{eff}$ produced in the Lab-extruder ought to reinforce the reasons for its unsatisfactory mixing performance mentioned in Section 1. On the same simplifying assumptions as for calculation of $\dot{\gamma}_{eff}$ in the internal mixer, $\dot{\gamma}_{eff}$ in the screw channel of the single-screw extruder is calculated, based on the screw extrusion theory[15,38–41] and melt flow characteristics on extrusion[42,43]. The results indicate that $\dot{\gamma}_{eff,max}$ for the Lab-extruder could be of the order of $10^2\ s^{-1}$ and definitely lower than $\dot{\gamma}_{eff,max}$ attained for the internal mixer used here, $174\ s^{-1}$ (see equation (2)). As far as compared among mixers with similar geometry, the shear strain, the product of the shear rate and the residence time for shearing, is one of the quantitative criteria to assess the degree of mixing[12–14,18,39,44–47]. As the geometry of mixing devices is different between the internal mixer and the Lab-extruder, the shear strain might not be very helpful to distinguish the quantitative mixing performance between the two mixers. However, it is natural that the internal mixer should give a better degree of mixing than the Lab-extruder since the former imposed much more shear strain than the latter. In the mixing experiment here, the average shear strain produced in the former was over several times as much as that in the latter, since the former took much more residence time in addition to a higher $\dot{\gamma}_{eff,max}$.

*Compression moulding.* The pressing machine and moulding conditions were the same as those employed before[8,9]. The mixed materials (irregular disk-shaped lumps) were dried at 80°C for 4 h, and then compression moulded at 200°C for 5 min into three types of rectangular plaques of different thicknesses (150 mm × 150 mm × 3.0 mm, 4.0 mm and 6.0 mm), followed by cooling hot moulds. Cooling was carried out by running cold water through pipes in mould clamping plates of the pressing machine in order for the mould temperature to drop down to 50°C in 3 min. The compressive direction was identical to the thickness direction of the plaques. *Figure 2* shows the geometry of a moulded plaque. For convenience the axes of coordinates crossed at right angles are fixed on the plaque so that the $X$ direction is identical to the compressive direction and that the $XZ$ plane is parallel to the operating side and also the backside of the pressing machine used here. The directional definition on the plaque relative to the pressing machine is indispensable because of an appropriate treatment for the significant mechanical anisotropy of KR05/MS-200 blends, which occurs when they are compression moulded on the pressing machine used here under above-mentioned moulding conditions[9]. The

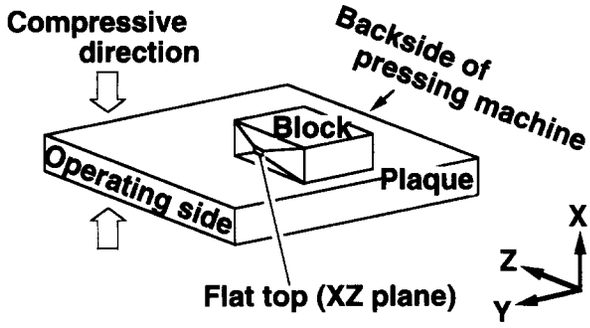


**Figure 2** Diagram showing a pyramid-shaped piece cut from an compression-moulded plaque. The *X* axis is fixed in the compressive direction. A flat top on the piece was made for microtoming parallel to the *XZ* plane

mechanical properties of the blends vary depending on the machining direction of the test bars parallel with the *YZ* plane of the moulded plaques. Such mechanical anisotropy arises from the orientational anisotropy of microdomain structure of the KR05 lamellar phase of the blends[9]. This could be induced by non-uniform cooling due to unbalanced layouts of the watercooling pipes embedded in mould clamping plates of the pressing machine[32]. The anisotropic characteristics of the blends were discussed previously[9], and are not discussed in this paper.

Compression-moulded plaques were machined along the *Y* and the *Z* directions with metal templates into impact (4.0 mm in thickness), tensile (3.0 mm) and flexural (6.0 mm) test bars, respectively. The longitudinal directions of the bars were normal to the compressive direction. The flexural test bars were also used for deflection temperature measurement under flexural load (DTUL). All test bars were cut from the inner regions far from the sides of these plaques, so that one could ignore the end effect of microdomain structure on mechanical properties. This effect is based on the disturbance of microdomain structure due to chaotic flow near the mould walls during compression moulding.

As-received KR05 was also kneaded in the internal mixer and processed to make test bars in a similar way.

*Mechanical tests*

The notched Izod impact strength was measured at 23°C according to ASTM D256 using a pendulum type tester. Tensile and three-point loading flexural tests were performed on a conventional Instron testing machine at 23°C according to ASTM D638 and ASTM D790, respectively. The DTUL was measured under a maximum fibre stress of 1820 kPa according to ASTM D648. Two sets of test bars were machined from compression-moulded plaques in the two respective directions which meet each other at right angles, namely, in the *Y* and the *Z* directions. Mechanical properties of the two sets were examined considering the mechanical anisotropy of compression-moulded KR05/MS-200 blends. However, anisotropy of the impact strength is only shown in this paper for reference (see Section 3.3), since such mechanical anisotropy has been already examined and discussed[9]. For the other mechanical properties, the resultant data for both directions were averaged to compensate the mechanical anisotropy.

*Examinations of morphology*

Morphology of neat KR05 and KR05-enriched KR05/MS-200 blends was observed by transmission electron microscopy (TEM). Morphological evaluation of the mixtures quenched after melt mixing in the internal mixer and their compression mouldings was performed. Pyramid-shaped pieces were cut from inner regions of internally-mixed materials (irregular disk-shaped lumps) and compression-moulded plaques (4.0 mm thick). Anisotropic characteristics of the lumps were not considered, since there is little probability of such anisotropy because of no large directivity of the shear and elongational flows in the internal mixer. On the contrary anisotropic characteristics of compression mouldings had to be considered since significant orientational anisotropy of the KR05 lamellar matrix arose during compression moulding on the pressing machine under the moulding conditions adopted here[9,32]. The apexes of the pieces were machined from regions close to the geometrical centres of the compression-moulded plaques and were cut off to expose surfaces of the XZ plane on the resultant flat tops, as shown in *Figure 2*. The microscopic surfaces for morphological observation were always made at fixed positions close to the geometrical centres of the plaques, and on the specified plane (the *XZ* plane of the plaques). When comparison among the blends with various compositions was made of the morphology viewed on such surfaces, the effects of morphological anisotropy could be ignored since these surfaces were subjected to much the same cooling history during cooling the plaques on the pressing machine used here. They were at the same geometrical position relative to the layouts of water-cooling pipes embedded in the mould clamping plates of the machine.

After staining treatment with a 2% aqueous solution of osmium tetroxide, ultrathin sections (500 to 900 Å in thickness) were microtomed on flat tops of the pieces using an LKB microtome with a diamond knife. Sections were observed by using a Hitachi H700 TEM at an accelerating voltage of 100 kV, and routine magnifications 15 000 ×, 30 000 × and 100 000 × were used.

*MS-200 domain size analyses*

The MS-200 domain size and distribution in the KR05-enriched KR05/MS-200 blends, KR05/MS-200 (90/10), (85/15), (80/20), (75/25) and (70/30), were examined, to find the appropriate diameter range for toughening of the blends. Sectional images were acquired from TEMs of the blends with a Toshiba TOSPIX image processor. About 150–600 MS-200 domains for each blend were scanned with an image analyser of Toshiba Data System 600 to determine their profile size distribution. Most of the outlines of the domains on the micrographs looked elliptical rather than circular since ultrathin sections including rubbery polymers are often compressed in the sectioning direction by shear produced at a knife edge on microtoming at the room temperature[48,49]. It is suggested that the actual MS-200 domains in the blends prior to microtoming could be spherical. The computed diameter of the imaginary circle as large as the ellipsoid in area was regarded as the diameter specific to the ellipsoid for calculation of the domain size and its distribution.

The three-dimensional size distribution of the MS-200 domain in the blends was estimated by the profile size distribution from microtomed ultrathin sections. Many studies have been carried out to predict the three-dimensional size and its distribution from the profile size analysis[50–55], and the resultant theories have been applied to actual two-phase material systems[50,51,56–58]. The method proposed by Mihira and coworkers[50,51] was employed here

since a rough approximation to the three-dimensional size distribution can be obtained from the corresponding profile size distribution of the domains without complexity of computer-aided statistical calculation.

## RESULTS AND DISCUSSION

### *Morphological change on melt processing*

*Figures 3 and 4* show morphologies of neat KR05 quenched after kneading in the internal mixer and the corresponding compression moulding, respectively. The morphology in *Figure 3* was viewed at core regions of irregular disk-shaped lumps. That in *Figure 4* was observed on sections microtomed parallel to the compressive direction on the XZ plane at core regions of 4.0 mm thick plaques (see *Figure 2*). The compressive directions are shown by the arrows on the micrographs. *Figure 3*b and *Figure 4*b are higher magnification views of *Figure 3*a and *Figure 4*a, respectively. The KR05 morphologies show lamellar phase separation between the PS and the PB phases as reported previously [32]. The kneaded KR05 (*Figure 3*) shows incomplete lamellae, since many parts of the PB lamellae are disconnected in the PS matrix phase, which must have been formed in the non-equilibrium state on rapid water cooling just after completion of kneading. The lamellae look chaotically corrugated since kneading in the internal mixer did not subject KR05 to anisotropic stress large enough to induce straightforward lamellar orientation, and the disarrayed microdomain structure in the melt was

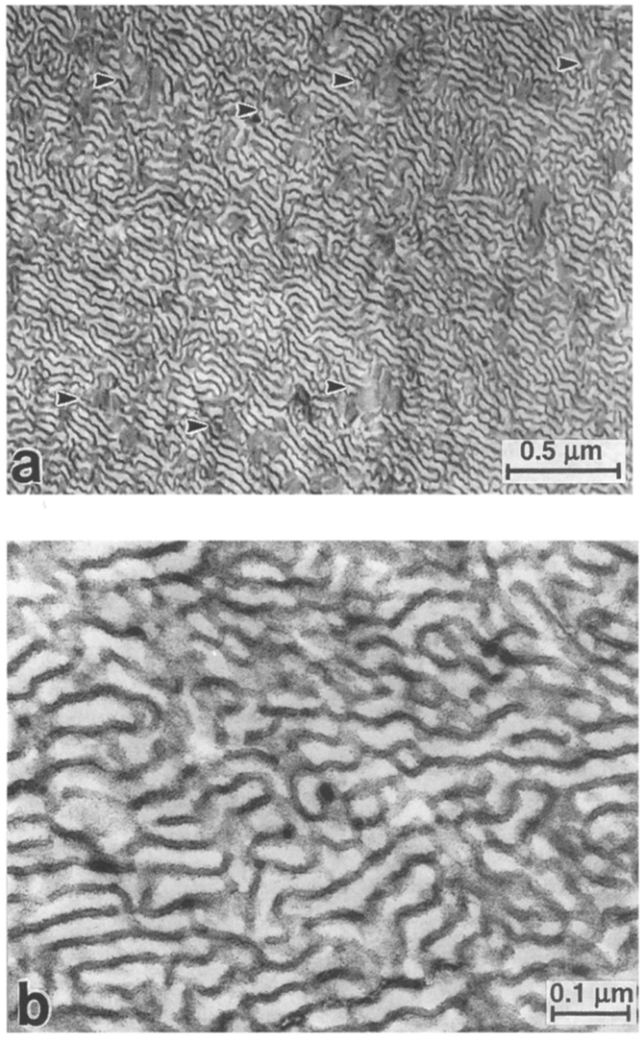


**Figure 3** TEMs of internally-kneaded KR05. (b) is a higher magnification view of (a). Arrowheads on (a) indicate microscopic regions where microtoming was done along or obliquely for lamellar orientation directions

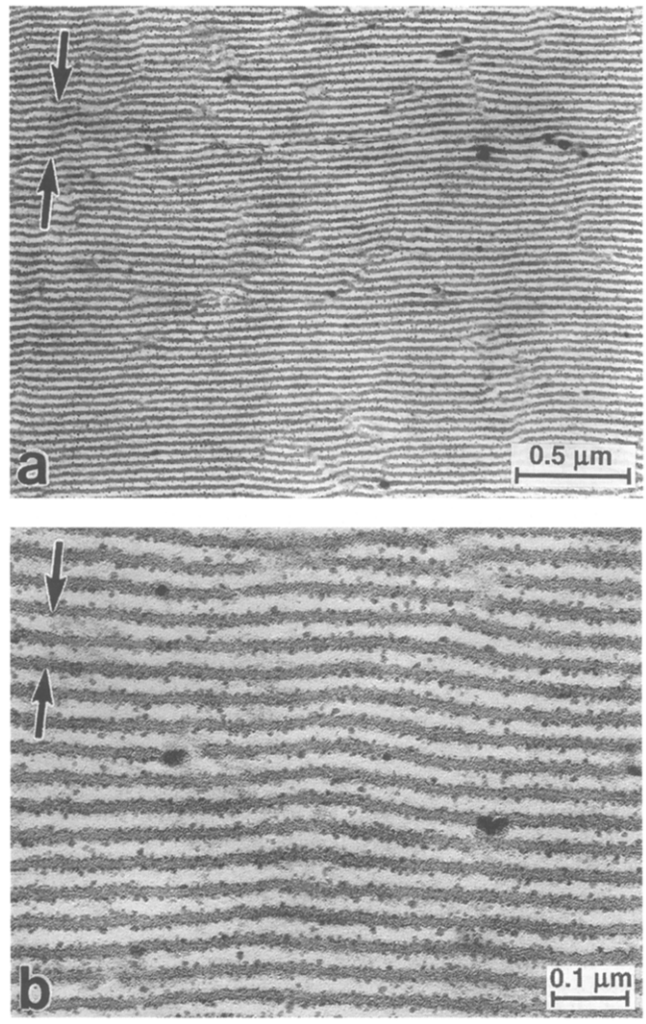


**Figure 4** TEMs of a compression moulding of internally-kneaded KR05. (b) is a higher magnification view of (a). Morphology was viewed on sections microtomed on the *XZ* plane (see *Figure 2*). The arrows on the micrographs show the compressive directions

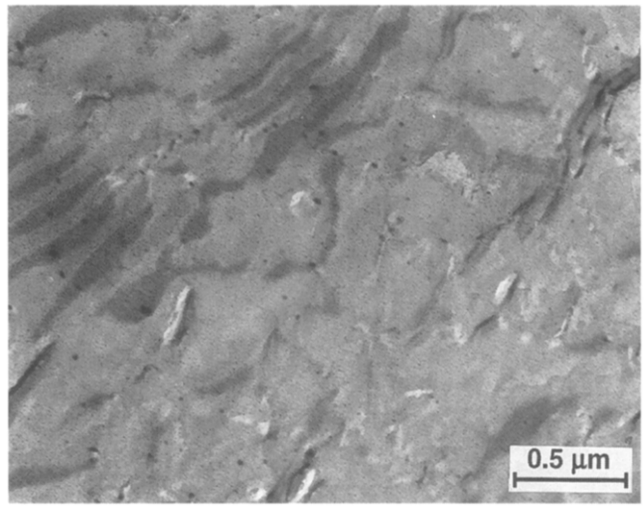


**Figure 5** TEM of a compression moulding of internally-kneaded KR05 showing local and minor morphology without clear stripe pattern of KR05 lamellae on the *XZ* plane

mostly freezed on the subsequent rapid cooling. The three-dimensional disarray of the lamellar orientation is inferred easily from the morphology studded with microscopic regions showing dim or no stripe patterns of the lamellae, which were found in places on the microtomed sections as indicated by arrowheads in *Figure 3*. Such regions must be sectional views microtomed roughly along or obliquely for the orientation direction of the lamellae stained by osmium tetroxide.

On compression moulding of the lumps the majority of the lamellar microdomain structure in the resultant plaque of neat KR05 was rearranged and turned orderly, as viewed in *Figure 4*, which is the representative morphology on the XZ plane of the plaque. However, the local and minor morphology without clear stripe pattern of the lamellae was also found on the *XZ* plane, as viewed in *Figure 5*. Microscopic regions with such morphology should be sectional views microtomed roughly along the lamellar stratification direction or obliquely for that direction since the intervals between neighbouring stained lamellae in *Figure 5* look very wide. Note that this disarray of the lamellar orientation in places could be induced by non-uniform cooling on the pressing machine used here, as discussed previously[32]. The orderly lamellar formation as viewed in *Figure 4* should be due to the kinetic history on compression moulding. At the melt temperature of 180–200°C employed during melt processing here, KR05 should be phase-separated in the melt state, and the memory of the lamellar morphology would not be initiated, and only reorientation and lattice ordering of the lamellae could occur[32]. When compression moulded, orientation and lattice ordering of the KR05 lamellae could be developed well before complete solidification. The residual strain in the molten texture of the kneaded KR05 could be relaxed well on 5-min pressing at 200°C. On subsequent 3-min cooling down to 50°C the majority of the molten lamellae could be reoriented to ordered stratification in the mould, since the average diffusion distance of molten KR05 molecules for the first 30 s on cooling should be over the undulation size of the lamellar disorder even at the region only 0.5 mm in depth from the surface of a 4.0 mm thick plaque[9].

Comparison between lamellar thicknesses before and after compression moulding has suggested that the PB lamellae thickened without perceivable expansion of the PB–PB interlamellar distance (the sum of the PB and the PS lamellar thicknesses) on compression moulding, and thus volume fraction of the PB lamellae looks as if it increased through the moulding process. Such dilatational change of the lamellar thickness should occur due to the self-diffusion of block copolymer molecules as a result of their microbrownian motion above the $T_g$ of PS[59]. During compression moulding, the spatial distribution of chemical junction points between the PB and the PS blocks through the PB–PS interface could become broader, and consequently interfacial thickness could increase as the molecular diffusion developed. The apparent volume increase of the PB phase (more exactly, that of the $OsO_4$-stained region) should result, since $OsO_4$ stains not only the PB phase itself but also the PB-enriched parts of the thickened PB–PS interface. The lamellar thickening on compression moulding strongly suggests that the microdomain structure viewed in *Figure 3* is in the thermodynamic non-equilibrium state.

*Figures 6 and 7* show morphologies of KR05/MS-200(70/30) blend quenched after melt mixing in the internal mixer and the corresponding compression moulding, respectively. *Figures 6 and 7* were taken in the same way as *Figures 3 and 4*, respectively. The compressive directions are shown by the arrows on the micrographs of *Figure 7*. *Figure 6*b and *Figure 7*b are higher magnification views of *Figure 6*a and *Figure 7*a, respectively. The blend exhibits the island-matrix morphology in which unstained MS-200 domains are phase-separated from the KR05 lamellar matrix. Similar phase separations were seen in extrudates of the KR05/MS-200 blends and their mouldings[7,8]. The morphology seen in *Figure 6* is characterized by incomplete formation of KR05 lamellae and ill-shaped MS-200 domains. Defective lamellae should result from little microdomain relaxation on non-equilibrium rapid cooling just after mixing. There are many ill-shaped MS-200 domains in the gourd-like shape with pinched-in portions in the blends taken out of the internal mixer. Such domain shape presumably reflects either the dynamic equilibrium state of the molten domain morphology under shear in the internal mixer, or the morphological features in course of form relaxation or coalescence of the molten domains after cessation of shear. The author thinks that this should be due to the former, since the domains could neither relax nor coalesce significantly on rapid cooling in water just subsequent to internal mixing. During long internal mixing the morphology of the polymer melt being mixed could be dynamically equilibrated. Before reaching the steady state the induced shearing force deformed the dispersed MS-200 phase into elongated domains which

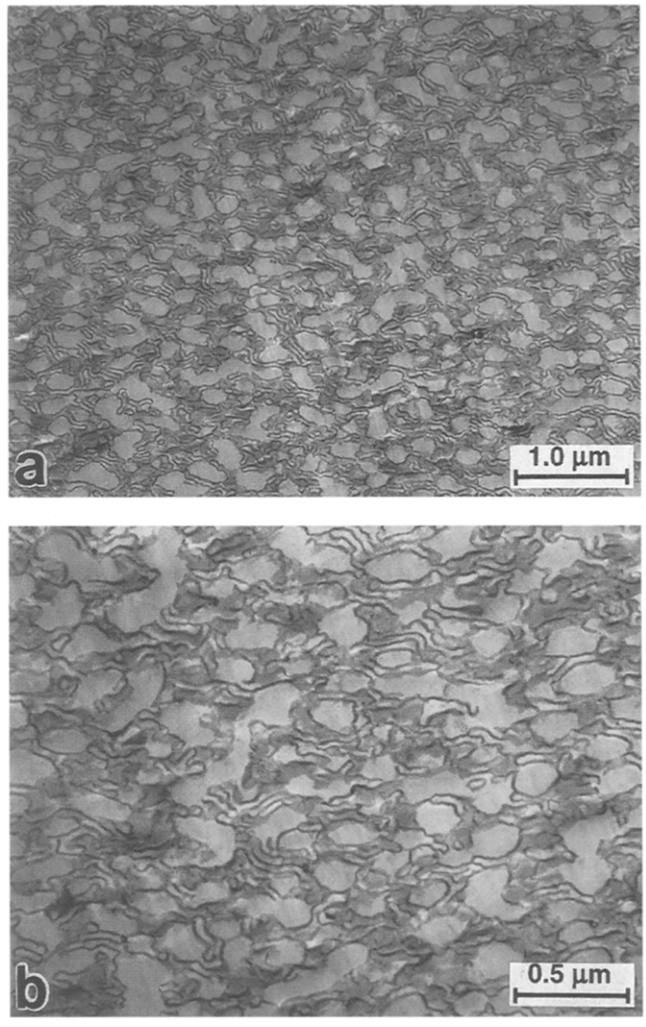


**Figure 6** TEMs of internally-mixed KR05/MS-200(70/30). (b) is a higher magnification view of (a)

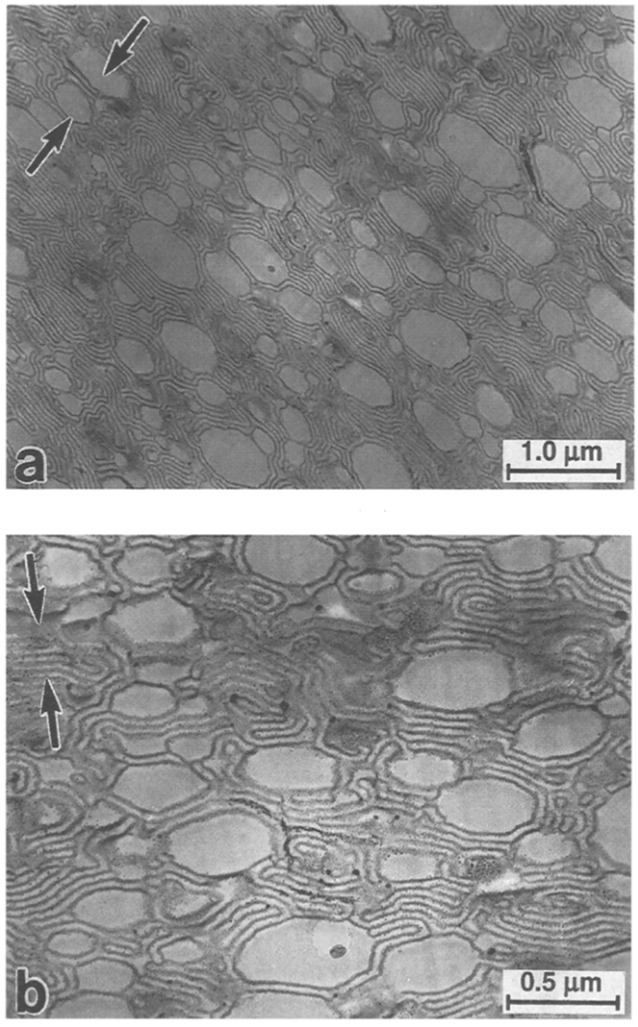


**Figure 7** TEMs of a compression moulding of internally-mixed KR05/MS-200(70/30). (b) is a higher magnification view of (a). Morphology was viewed on sections microtomed on the *XZ* plane (see *Figure 2*). The arrows on the micrographs show the compressive directions

were constricted in the middle spontaneously until their breakdown. The constrictions were induced by microbrownian motion, or by local changes in the shearing pattern due to variation in the relative positions of the surrounding domains[60]. At the steady state apparent domain-size reduction did not occur any more, and actually the total shearing force on the domains equalled the interfacial tension to the matrix polymer, which is the force retracting the elongated domains[60]. The gourd-shaped MS-200 domains could be formed in the steady state when the rate of deformation followed by constriction in the middle of the domains was balanced with their retraction rate.

Comparison between MS-200 domain size before and after compression moulding (*Figures 6 and 7*) has suggested that the blends were demixed perceptibly during compression moulding. Coalescence of the domains occurred on 5-min static hot pressing, which is inconsistent with no appreciable demixing occurred on compression moulding of the KR05/MS-200 blends extruded with the Lab-extruder[8]. This discrepancy would not result primarily from difference in the degree of mixing attained for KR05/MS-200 blends between the internal mixer used here and the Lab-extruder. The principal reason for such inconsistency could be in the following. Suppose $L_{ss}$ is defined as the wall-to-wall distance between two neighbouring MS-200 domains dispersed in the KR05 matrix. Compared with the $L_{ss}$ of the internally-mixed blends, the corresponding extruded blends show comparatively large $L_{ss}$ between the MS-200 domains which neighbour along the transverse direction (i.e. the direction normal to the extrusion direction) since most of the domains are thin in the transverse direction due to their slender elongation in the extrusion direction. Therefore, the domains neighbouring along the transverse direction in the extruded blends could coalesce much less than the domains neighbouring in the internally-mixed blends. Another reason is larger domain retraction on compression moulding of the extruded blends than of the internally-mixed blends. $L_{ss}$ between the MS-200 domains which neighbour along the extrusion direction in the extruded blends would not decrease significantly on compression moulding since strong retracting tendency of the domains highly elongated in the extrusion direction resists being coalesced along the extrusion direction.

The KR05 lamellae of the blends melt mixed in the mixer (see *Figure 6*) are corrugated and the MS-200 domains vary in shape. In contrast, the compression-moulded blends (*Figure 7*) show orderly morphology in which KR05 lamellae are stratified regularly and MS-200 domains look spherical. This orderliness should be due to the kinetic history on compression moulding. At the melt temperature of 180–200°C employed during melt processing here, KR05/MS-200 blends should be phase-separated in the melt state between the PB and the PS phases in KR05, and between the KR05 and the MS-200 phases[7,32]. The memory of the separation would not be lost and only relaxation and reorientation of each phase could occur[8]. When compression moulded, each molten phase could be relaxed well on 5-min hot pressing, and KR05 lamellae should be rearranged to ordered stratification on subsequent cooling in the mould before complete solidification[32].

*Degree of internal mixing*

In order to control the size of the MS-200 dispersed domain, the blend composition was varied for internal mixing. It has been expected that the size could change significantly with nothing but the formula change of the blend composed of the two commercially-available polymers KR05 and MS-200, since it is proved theoretically that for ordinary polymer blends the equilibrium domain size increases definitely with increasing volume fraction of inclusions[61].

*Figure 8* shows morphologies of compression mouldings of internally-kneaded KR05 and internally-mixed blends with the KR05-enriched composition. They were observed in the same way as *Figure 7* and their compressive directions are shown by the arrows on the micrographs. The compression-moulded blends have the island-matrix morphology, in which fairly uniform dispersion of MS-200 domains is achieved with ordered stratification of KR05 lamellae. MS-200 domain dispersion and size, and KR05 lamellar orderliness have been compared between compression mouldings of the blends after internal mixing and those after extrusion through the Lab-extruder. The latter blends were examined previously and referred to as 'once-extruded' blends after extruding the materials once and 'twice-extruded' blends after two-fold extrusion[8,9].

Once-extruded blends with the enriched composition of KR05 had the morphology with very poor degree of mixing, in which MS-200 inclusions were diverse greatly from submicrometres to more than ten micrometres in size and showed significantly biased distribution[7,8]. Once-extruded

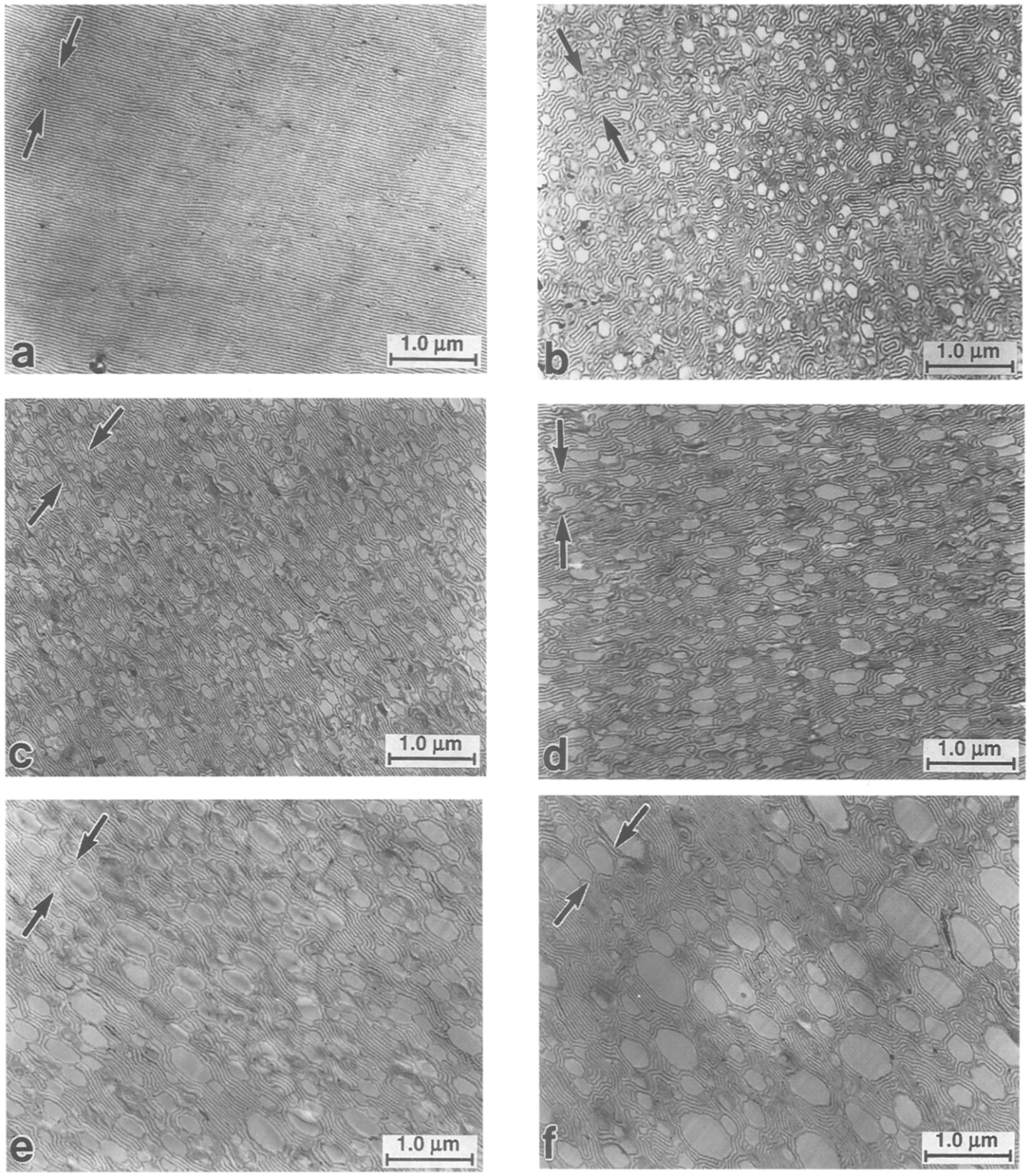


**Figure 8** TEMs of compression mouldings of internally-kneaded KR05 and internally-mixed KR05/MS-200 blends with the KR05-enriched composition: (a) KR05/MS-200(100/0); (b) (90/10); (c) (85/15); (d) (80/20); (e) (75/25); (f) (70/30). Morphology was viewed on sections microtomed on the *XZ* plane (see *Figure 2*). The arrows on the micrographs show the compressive directions

blends are definitely inferior to internally-mixed ones in degree of mixing, consequent on the inferiority of the Lab-extruder in mixing performance as mentioned in Sections 1 and 2. *Figure 9* shows morphologies of compression mouldings of twice-extruded KR05/MS-200(85/15) and (70/30) blends, which were viewed on cross-sections parallel to the *XZ* plane of the compression-moulded plaques in previous studies[8,9]. Compression mouldings of internally-mixed and twice-extruded blends with the same composition exhibit morphological analogy, in comparison between *Figure 8*c and *Figure 9*a for KR05/MS-200(85/15), and *Figure 8*f and *Figure 9*b for KR05/MS-200(70/30). Such analogy means that materials must be extruded twice through the Lab-extruder in order to attain a degree of mixing similar to that after the internal mixing employed here. Internally-mixed blends seem to have a

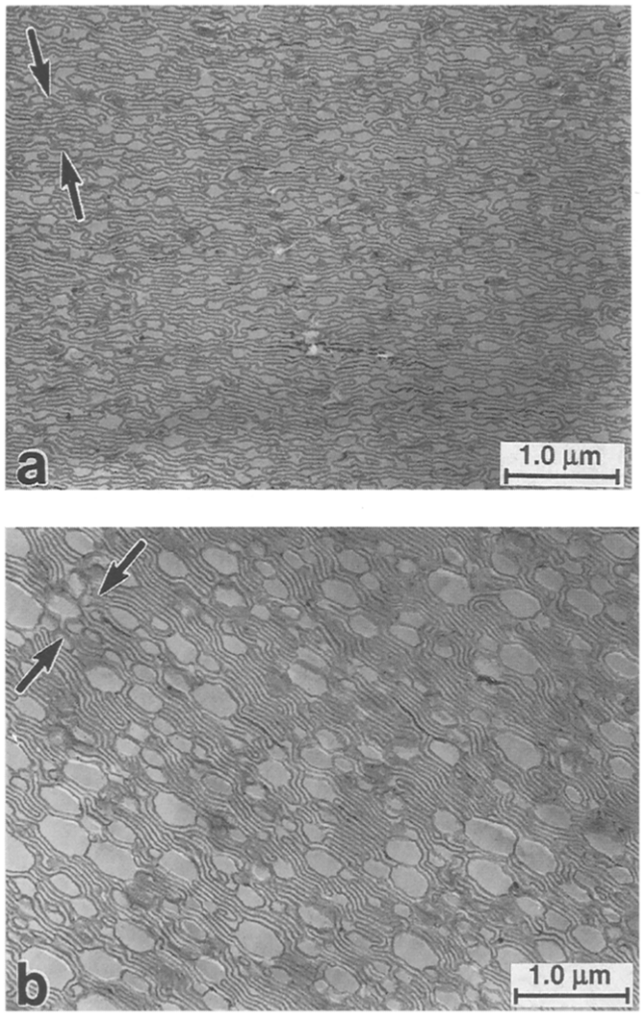


**Figure 9** TEMs of compression mouldings of twice-extruded KR05/MS-200 blends: (a) (85/15); (b) (70/30). Morphology was viewed on sections microtomed on the *XZ* plane (see *Figure 2*). The arrows on micrographs show the compressive directions

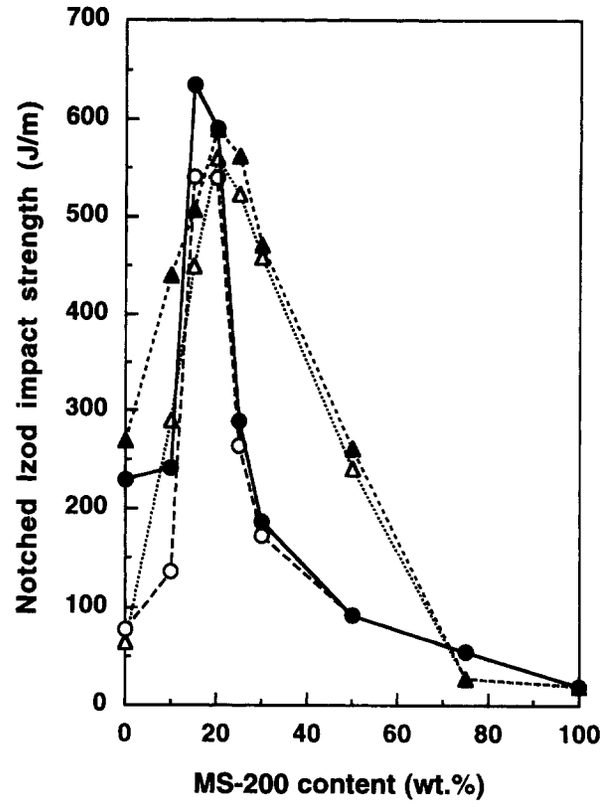


**Figure 10** Notched Izod impact strength of KR05/MS-200 blends plotted as a function of MS-200 content. Circular symbols represent the data for compression mouldings of internally-mixed blends. The data for compression mouldings of twice-extruded blends are reproduced from the previous paper[9], shown by triangular symbols. Solid and hollow symbols show the results from test bars machined in the *Z* and the *Y* directions which meet each other at right angles, respectively

slightly bigger MS-200 domains than twice-extruded ones with the same composition. Direct comparison in MS-200 domain size between internally-mixed lumps and extruded pellets is impossible because of the complete dissimilarity in the domain shape between the two mixtures (for the former spherical or gourd-like, and for the latter highly elongated). However, once they are compression moulded, the similarity in MS-200 domain shape between the two kinds of compression mouldings (see *Figures 8 and 9*) enables one to compare the rough degree of mixing in internally mixed lumps with that in extruded pellets, considering the perceivable coalescence of MS-200 domains to size growth on compression moulding of the internally-mixed lumps. The comparison suggests that degree of mixing in internally-mixed KR05/MS-200 blends could match roughly that in twice-extruded blends when allowances are made for the influence of coalescence during compression moulding for the former. Internal mixing could bring the degree of mixing comparable to that accomplished on screw extrusion as reported elsewhere[62,63].

The MS-200 domain of compression mouldings of the internally-mixed blends is a little coarser than that of twice-extruded blends with the corresponding composition. However, the former mouldings show a large toughness enhancement which parallels that of the latter mouldings, as discussed later.

Ten minute internal mixing here should be long enough to attain the equilibrium MS-200 domain size, which can be suggested from the following viewpoint. Dry-blended material pellets, which were not preheated, were fed onto the nip region between the hot rotors running in the chamber. For a couple of minutes after mixing began the monitored torque value fluctuated largely due to the unmolten pellet breakup. At a beginning stage of mixing the majority of power consumption of the mixing motor (*ca* 4.7 kJ for the first 2 min) could be used for the material temperature rise. If all the mechanical energy input was consumed to heat the material to be broken up, the temperature rise of *ca* 23°C resulted. This is partly responsible for the rapid temperature rise of the material. At an intermediate stage of mixing the torque stopped fluctuating and instead began decreasing rapidly as the molten phase grew. The large decrease of the torque must be consequent on the growth and the temperature rise of the molten phase, although the unmolten minor phase may still exist and suspend in the molten phase. After completion of melting, mixing could go into a final stage in which the torque decrease was gradually decelerated, and then the torque was being levelled off 7–9 min after mixing began. The constant torque value was reached at most in 10 min after mixing began. As long as the torque decreased, the overall viscosity of the polymer melt being mixed could decrease since the torque becomes a measure of the overall viscosity after complete melting[60,64]. The observed

deceleration of the torque decrease with time should correspond to that of the overall viscosity decrease as the time elapsed. At an earlier part of a final stage deceleration of the viscosity decrease might result from the deceleration of the melt temperature rise as the melt temperature increased and became closer to the chamber temperature of the mixer. However, at a later part of a final stage the viscosity decrease could be closely related to the MS-200 domain size reduction, since a certain extent of viscosity change of the whole system must occur as long as the dynamic change of the domain morphology lasts in the flow field. The viscosity levelling could correspond to the deceleration of the MS-200 domain size reduction as the MS-200 phase broke down and the resultant dispersed domains became gradually smaller to the equilibrium size. Therefore, the torque decrease of the melt here should be a good reflection of the domain size reduction. At a later part of a final stage the torque decreased more gradually with time since the MS-200 domain size reduction could be decelerated with time till the domain deforming force was equaling the domain retracting force (i.e. interfacial tension between KR05 and MS-200). The torque would be levelled off at equilibrium when breakdown and coalescence of domains were completely balanced. By monitoring torque values the author determined whether the equilibrium dispersion state of MS-200 domains was reached or not. Ten-minute mixing of KR05 with MS-200 here should be long enough to attain the equilibrium MS-200 domain size because the measured torque was always levelled off at most in 10 min after mixing began.

*Mechanical properties*

*Figure 10* shows the change and the anisotropy in the notched Izod impact strength of compression mouldings of the internally-mixed blends, together with these of the twice-extruded blends reproduced from the previous paper[9]. For the former KR05 is toughened remarkably by incorporation of MS-200, comparable to toughness enhancement for the latter. When a broad view of the impact behaviour is taken, the impact strength for the two cases exhibits much the same degree of synergistic improvement and traverses its maximum between 10 and 30 wt% MS-200, where the blends are composed of the ductile matrix. This analogous synergy effect must result from the morphological analogy between the two mouldings with the identical composition, as mentioned in the previous section. When impact stress is imposed on either moulding, excessive stress concentration which may cause destructive microcracks could be avoided by extensive microstructural changes with shear yielding of the lamellar KR05 matrix, cavitation in the PB phase and debonding in the KR05/MS-200 interfacial region[8].

When a close view of the impact behaviour is taken, however, the change in the impact strength with increasing MS-200 content is meaningfully different between the two mouldings. Respective sets of measured impact data, which were averaged to the values of the impact strength to be plotted on *Figure 10*, are scattered to a significantly small extent compared with the difference of the impact strength between the two mouldings with the same composition. The coefficient of variation (ratio of the standard deviation to the average value) for each set of measured impact data is small, of the order of 0.05 to 0.1. Anisotropy of the impact strength, which was discussed previously[9], is also meaningfully present in KR05-enriched blends for the similar reason. MS-200 content at which the maximum of the impact strength is traversed is smaller for the internally-mixed blends than for the twice-extruded blends. One of the reasons is that MS-200 content at which the most appropriate domain size for toughening is formed could be smaller for the former than for the latter, since a little coarser dispersion of MS-200 domains was obtained for the former as mentioned in the previous section.

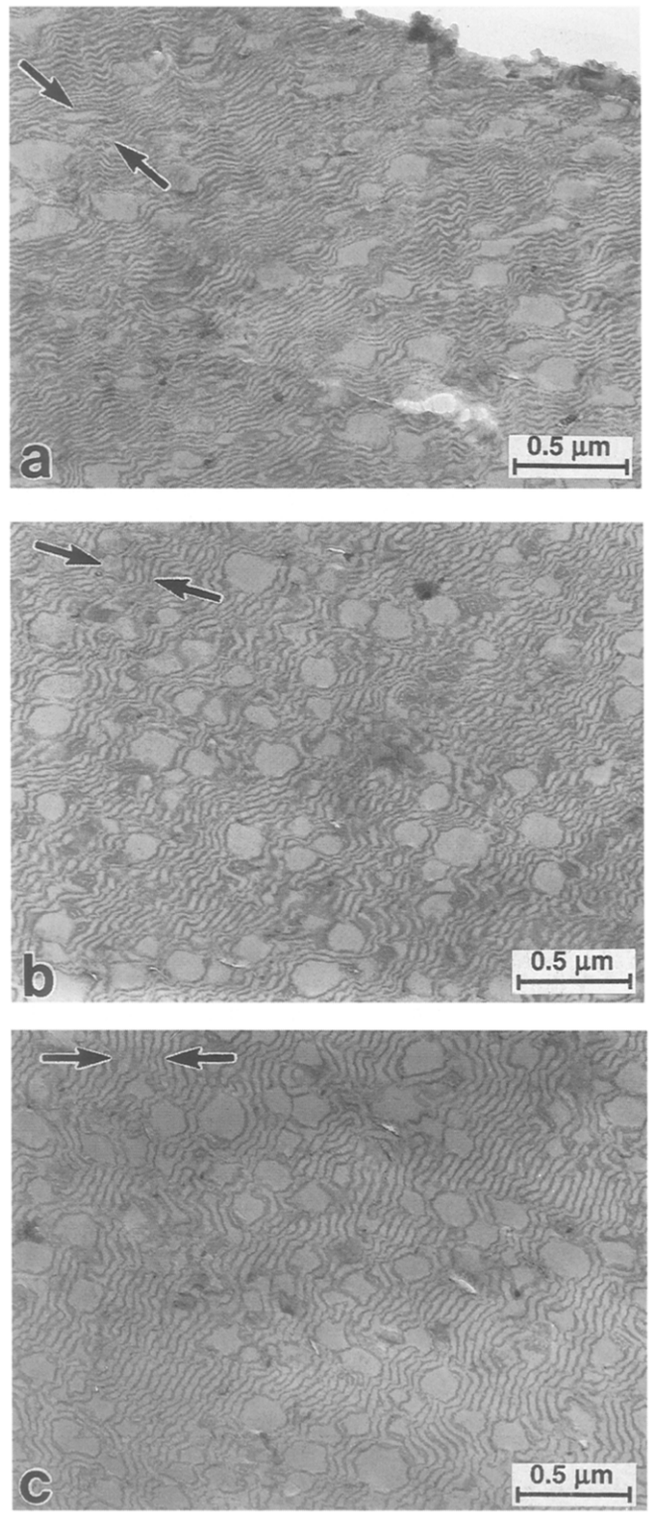


**Figure 11** TEMs of a compression moulding of internally-mixed KR05/MS-200(85/15) blend after Izod impact testing. Morphology was viewed on a cross-section microtomed on the *XZ* plane (see *Figure 2*). The arrows on the micrographs show the compressive directions. (a) was taken perpendicular to the fracture surface as seen on the micrograph; (b) *ca.* 90 μm in depth away from the fracture surface; (c) *ca.* 300 μm in depth away from the fracture surface

The curve for the former has a sharper peak around 20 wt% MS-200. In the MS-200 content range over 20 wt% MS-200, compression mouldings of the internally-mixed blends are inferior to those of the twice-extruded blends in the impact strength. Such difference must result from the difference in distribution of the MS-200 domain size between the two kinds of mouldings. The melt mixing method and the composition of polymer blends are very influential in the resultant size distribution of dispersed domains, and if any, their agglomeration[65,66]. For KR05-enriched KR05/MS-200 blends here, processing-induced differences in domain size distribution must be important. Far-reaching distribution of the domain size would be more responsible than the distribution in much smaller regions five by five micrometres as viewed on the micrographs of *Figures 8 and 9*. *Figure 11* shows morphologies of a compression moulding of internally-mixed KR05/MS-200(85/15) blend after Izod impact testing. *Figure 11*a was taken on the *XZ* plane of the test specimen and perpendicular to the fracture surface as seen on the micrograph. *Figure 11*b and c were taken *ca* 90 and *ca* 300 $\mu$m respectively below the fracture surface on the same cross-section as for *Figure 11*a. On *Figure 11*a and b KR05 lamellae are more undulated and show one-sided expansion of lamellar spacing of the rubbery phase as a result of their shear yielding on fracture[8]. Analogy of the MS-200 domain size and its distribution among *Figure 11*a, b and c taken far away from one another has revealed that the domain size distribution seems to be similar in fairly extensive regions in the moulded plaques. Therefore, considerably uniform distribution of the domains on large scales over a few hundred micrometres must be attained. This result is reproducible with other cross-sections of compression mouldings of internally-mixed KR05/MS-200(85/15) blends. On the contrary, compression mouldings of twice-extruded KR05/MS-200(85/15) blends showed definitely uneven distribution of the MS-200 domain size on extensive scales[8]. In the mouldings the domain size at some microscopic regions was several times as large as that at some other regions far away, which could result from heterogeneity of degree of mixing still left in twice-extruded blends. Consequent on this discussion, difference in far-reaching distribution of the domain size should be one of the principal reasons to determine impact behaviour of the blends. Toughening of many blends strongly depends on the distributional features of dispersed domains as instanced in the following. The uniform domain size is more effective than the heterogeneous size in toughening of the blends with the pseudoductile matrix, such as the blends composed of the nylon matrix and rubbery inclusions[67]. On the other hand the bimodal-size distribution is advantageous to toughening of the blends with the brittle styrene–acrylonitrile copolymer (SAN) matrix and rubbery inclusions[68].

*Figure 12* shows the tensile strength of compression mouldings of the internally-mixed blends, together with that of the twice-extruded blends. The flexural modulus of those mouldings is shown in *Figure 13*. DTUL of these mouldings is compared in *Figure 14*. The data for the twice-extruded blends are reproduced from the author's previous paper[8]. For these rigidity-related properties, two sets of the data for test bars machined in the *Y* and the *Z* directions, which meet at right angles with each other, were averaged to compensate the mechanical anisotropy and the averaged values appear on *Figures 12–14*. Compression mouldings of internally-mixed blends roughly match the corresponding

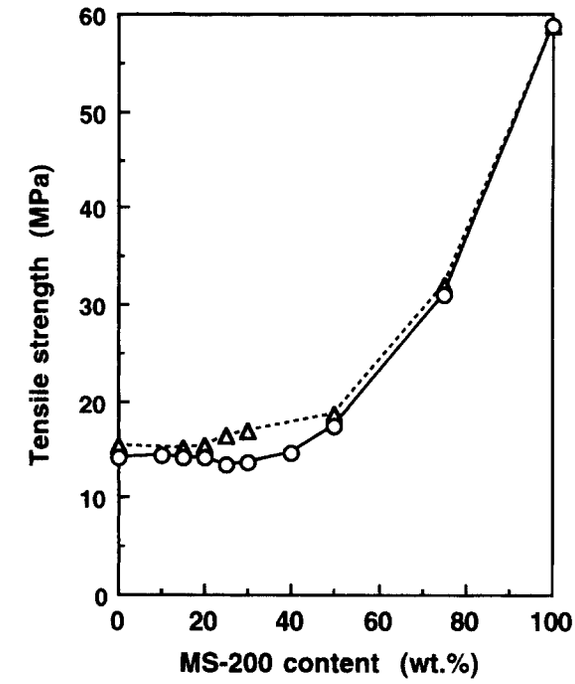


**Figure 12** Tensile strength of compression mouldings of internally-mixed KR05/MS-200 blends plotted as a function of MS-200 content. Circular symbols represent average values of the data obtained from two sets of test bars machined in the two respective directions, the *Y* and the *Z* directions which meet each other at right angles, so that anisotropy of the tensile strength is compensated. The averaged data for compression mouldings of twice-extruded blends are reproduced from the previous paper[8], shown by triangular symbols

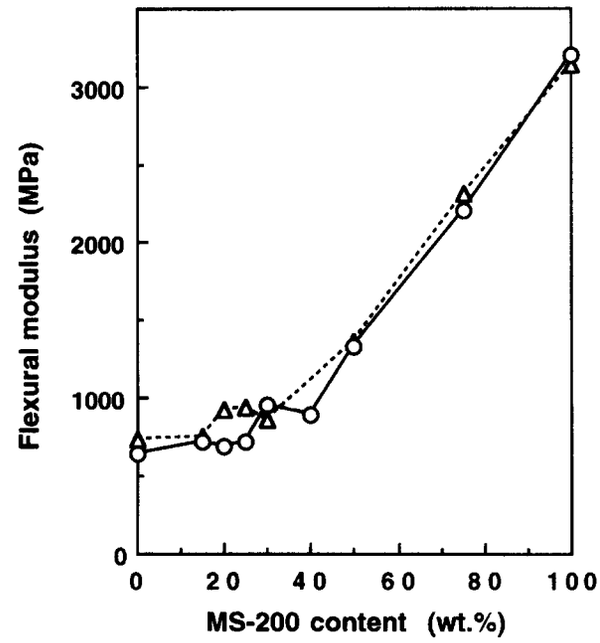


**Figure 13** Flexural modulus of compression mouldings of internally-mixed KR05/MS-200 blends plotted as a function of MS-200 content. Circular symbols represent average values of the data obtained from two sets of test bars machined in the two respective directions, the *Y* and the *Z* directions, which meet each other at right angles, so that anisotropy of the flexural modulus is compensated. The averaged data for compression mouldings of twice-extruded blends are reproduced from the previous paper[8], shown by triangular symbols

mouldings of the twice-extruded blends for these properties. This similarity could be due to the morphological analogy between the two mouldings with the identical composition, as mentioned in the previous section.

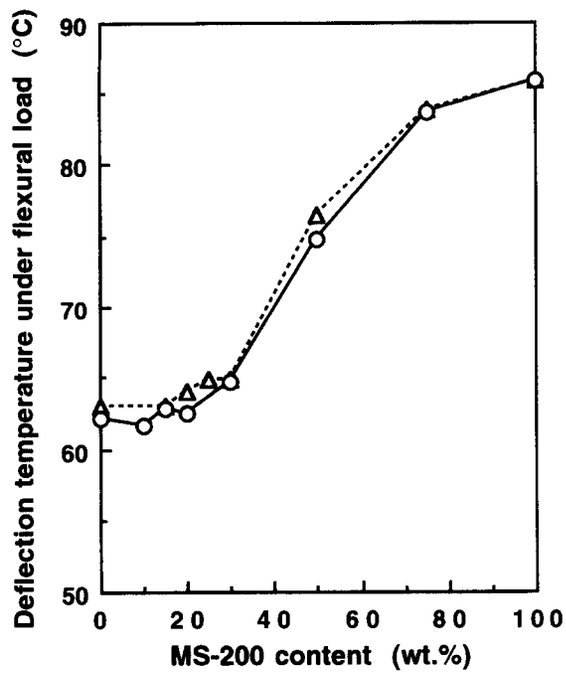


**Figure 14** Deflection temperature of compression mouldings of internally-mixed KR05/MS-200 blends under flexural load (DTUL), plotted as a function of MS-200 content. Circular symbols represent average values of the data obtained from two sets of test bars machined in the two respective directions, the *Y* and the *Z* directions which meet each other at right angles, so that anisotropy of DTUL is compensated. The averaged data for compression mouldings of twice-extruded blends are reproduced from the previous paper[8], shown by triangular symbols

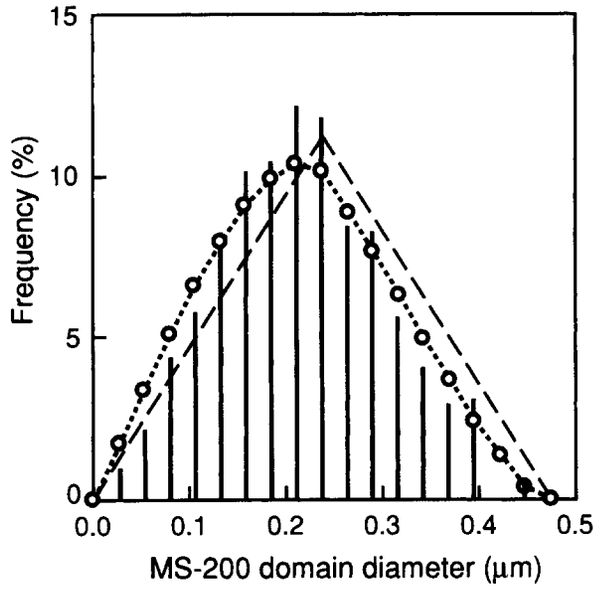


**Figure 15** MS-200 domain size distributions for compression mouldings of internally-mixed KR05/MS-200(85/15) blend. Profile size distribution observed on TEM sectional images is exhibited in a histogram. The dashed line shows three-dimensional distribution of the spherical domain diameter computed with the observed profile size distribution. The open circles traced by a dotted curve show profile size distribution calculated with the three-dimensional distribution function. The graduation of the horizontal axis is common to the profile and the spherical size of the MS-200 domain

*Domain size and distribution*

*Figures 15 and 16* show size distributions of the MS-200 domain for compression mouldings of internally-mixed KR05/MS-200(85/15) and (70/30) blends, respectively. Profile size distributions were examined with contour circles of MS-200 domains in sectional images of the blends seen on the TEMs, and are shown in histograms. Three-dimensional distributions of the spherical domain diameter were estimated on a basis of the observed profile size distributions according to the theory proposed by Mihira *et al.*[50,51], and are shown with dashed lines. Among the categories representative of the three-dimensional distribution proposed[50,51], the suitable pattern was applied in course of the distributional estimation for each blend. For the KR05/MS-200(85/15) blend the MS-200 domain could be dispersed roughly according to the triangular pattern, and for the (70/30) blend the number of the domain might decrease with increasing the diameter of the spherical domain in an approximately linear regime (the linear decrease pattern). The graduation of the horizontal axis is common to the diameter of the circular domain on the profile and that of the spherical domain. One might wonder if the three-dimensional distributions of the spherical domain diameter would be estimated into too simple patterns to represent the actual distributions, which would not be shown in such a triangular or linear decrease pattern with increasing the diameter. However, the author thinks that such simplicity should be incidental to the simplified computational procedure to approximate the actuality very roughly, and that the result should not deviate largely from the actuality. In order to confirm adequacy of the estimated three-dimensional distribution functions, profile size distributions have been calculated with these functions and plotted with open circles traced by dotted curves in the figures for comparison with observed profile size distributions. The observed profile size distribution (histogram) and the corresponding calculation (dotted curve) are in rough agreement for the two blends. Therefore, the estimated patterns of the three-dimensional distribution should be rough projections of the actual distributions. *Figure 17* shows the calculated three-dimensional distribution of the MS-200 domain size for compression mouldings of several internally-mixed KR05/MS-200 blends with the KR05-enriched composition. The number of MS-200 domains per unit volume (1 $cm^3$), which is termed the number density here, is plotted as a function of the spherical domain diameter. Among the blends examined here those with smaller MS-200 content (KR05/MS-200(90/10), (85/15) and (80/20)) show a triangular distributional pattern of the domain diameter, while the distributional pattern of KR05/MS-200(75/25) and (70/30) are based on a linear decrease with increasing domain diameter. The computed patterns could be rough traces of the actual distributions with some deviation from the actuality. It was strongly suggested that in KR05/MS-200 blends regions with MS-200 domains over a certain size could be fractured more easily under tensile stress than those with smaller domains[8]. Accordingly, toughness of the blends here could be correlated to the specific diameter ranges of the MS-200 domain, so that the range desirable for toughening can be estimated. The examination has revealed that the number density of the MS-200 domain of 0.3 to 0.5 $\mu$m in diameter should be influential. Highly toughened KR05/MS-200(85/15) and (80/20) blends with impact strength over 550 J $m^{-1}$ show higher number density of the domain of 0.3–0.5 $\mu$m in diameter than KR05/MS-200(90/10), (75/25) and (70/30) with impact strength less than 300 J $m^{-1}$. This means that highly toughened KR05/MS-200 blends could contain a lot of dispersed domains of 0.3–0.5 $\mu$m in diameter as far as only the blend composition was varied to change the

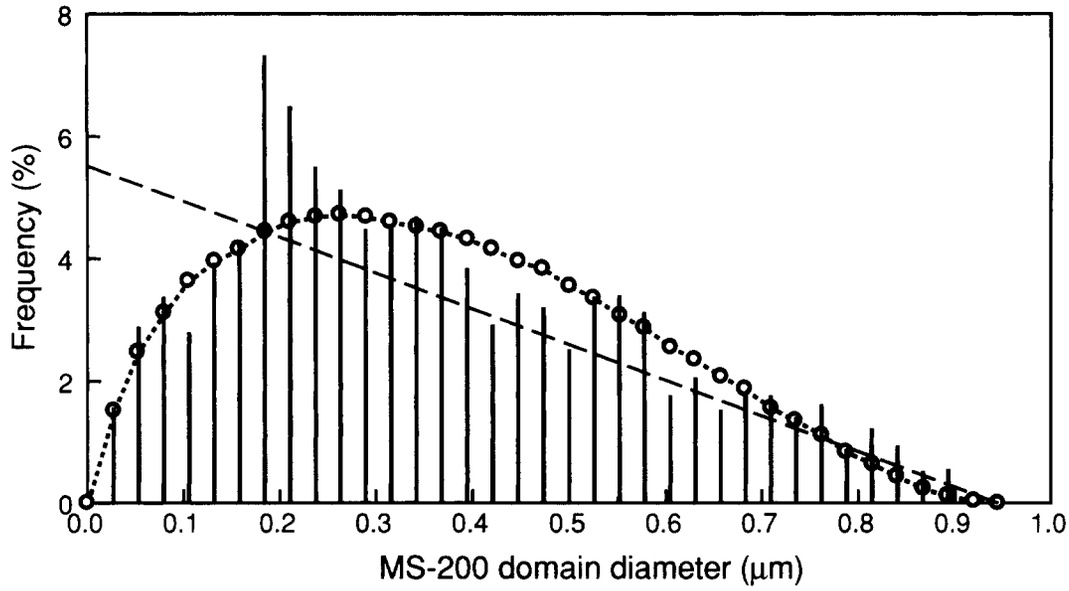


**Figure 16** MS-200 domain size distributions for compression mouldings of internally-mixed KR05/MS-200(70/30) blend. Profile size distribution observed on TEM sectional images is exhibited in a histogram. The dashed line shows three-dimensional distribution of the spherical domain diameter computed with the observed profile size distribution. The open circles traced by a dotted curve show profile size distribution calculated with the three-dimensional distribution function. The graduation of the horizontal axis is common to the profile and the spherical size of the MS-200 domain

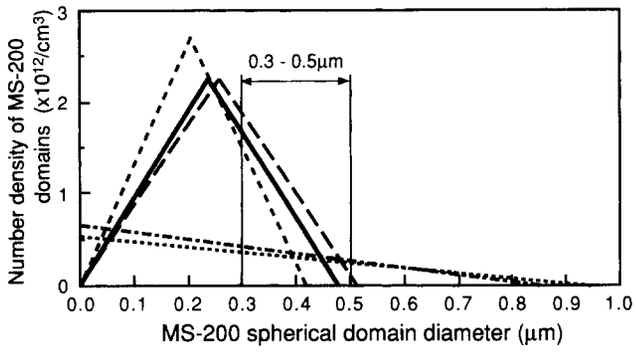


**Figure 17** Distribution of the number of the MS-200 domain per unit volume (1 $cm^3$), which is termed the number density here, plotted as a function of the spherical domain diameter for compression mouldings of internally-mixed KR05/MS-200 blends with the KR05-enriched composition: short dashed line (90/10); solid (85/15); long dashed (80/20); chain dashed (75/25); dotted (70/30)

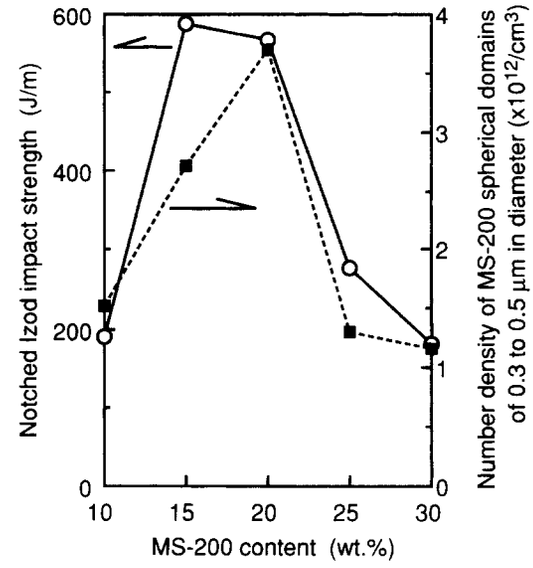


**Figure 18** Notched Izod impact strength (circular symbol), together with the number density of MS-200 domains of 0.3–0.5 $\mu$m in diameter (square symbol), plotted as a function of MS-200 content for compression mouldings of internally-mixed KR05/MS-200 blends with the KR05-enriched composition. Anisotropic impact data obtained from two sets of test bars machined in the $Y$ and the $Z$ directions, respectively, are averaged

domain size. *Figure 18* shows the notched Izod impact strength of the KR05-enriched blends together with the number density of the MS-200 domain of 0.3–0.5 $\mu$m in diameter, plotted as a function of MS-200 content. The anisotropic impact data obtained from two sets of test bars machined in the two respective directions (the $Y$ and the $Z$ directions; see *Figure 2*), are averaged for the figure. The two properties change in much the same manner as MS-200 content changes, which indicates the former should be related closely to the latter for the blends used here.

Morphological features of highly toughened KR05/MS-200 blends are given by incorporation of the discussion here with results from the previous studies[7,8]. When the blend composition was varied to control the size of the MS-200 domain, effective toughening of the blends could be obtained with the morphology that spherical MS-200 domains of 0.3 to 0.5 $\mu$m in actual diameter are densely dispersed in orderly lamellae of the ductile KR05 matrix.

## CONCLUSIONS

In the internally-mixed KR05/MS-200 blends KR05 exhibits lamellar structure alternating between the PB and the PS phases and phase separation from MS-200. The KR05-enriched blends which were cooled rapidly after internal mixing have many of MS-200 dispersed domains ill-shaped with constrictions in the middle, which could reflect the MS-200 domain morphology in the dynamic equilibrium state of the blends being melt mixed. When those blends were compression moulded, most of the gourd-shaped domains were relaxed well into spherical shape, and many of them coalesced to form the ordered morphology with regularly stratified KR05 lamellae. It has been found

that internal mixing is a powerful tool for melt mixing of KR05 with MS-200 since internally-mixed KR05/MS-200 blends should be roughly comparable to the twin-screw extruded blends in degree of mixing.

Ductile KR05 is a highly toughened by incorporation of brittle MS-200, and synergistic improvement of toughness is observed for compression mouldings of the internally-mixed blends with the composition from 10 to 30 wt% MS-200. When the blend composition was varied, MS-200 domain morphology to toughen KR05/MS-200 blends was examined. In this case KR05/MS-200 blends are toughened very effectively with the morphology that spherical MS-200 domains ranging from 0.3 to 0.5 $\mu$m in actual diameter are densely dispersed in the KR05 matrix composed of ordered lamellae.

## REFERENCES


1. Kurauchi, T. and Ohta, T., *J. Mater. Sci.*, 1984, **19**, 1699.
2. Fujita, Y., Koo, K.-K., Angola, J. C., Inoue, T. and Sakai, T., *Kobunshi Ronbunshu*, 1986, **43**, 119.
3. Angola, J. C., Fujita, Y., Sakai, T. and Inoue, T., *J. Polym. Sci., Part B: Polym. Phys.*, 1988, **26**, 807.
4. Koo, K.-K., Inoue, T. and Miyasaka, K., *Polym. Eng. Sci.*, 1985, **25**(12), 741.
5. Quingying, C., Wenjun, Z. and Fritz, H.-G., The Polymer Processing Society, Sixth Annual Meeting, Nice, France, ed. École Nationale Supérieure des Mines de Paris, France, 1990, P07-11 (Abstract).
6. Liu, T. M., Xie, H. Q., O'callaghan, K. J., Rudin, A. and Baker, W. E., *J. Polym. Sci., Part B: Polym. Phys.*, 1993, **31**, 1347.
7. Yamaoka, I., *Polymer*, 1995, **36**, 3359.
8. Yamaoka, I., *Polymer*, 1996, **37**, 5343.
9. Yamaoka, I., paper accepted for publication in Polymer.
10. Rauwendaal, C., *Polymer Extrusion*, Chapter 10 (Section 10.5). Hanser Publishers, New York, 1986.
11. Sakai, T., Hashimoto, N., Kobayashi, N., in *ANTEC'87 (Ann. Tech. Conf. Soc. Plast. Eng.)*, Los Angeles, ed. Society of Plastics Engineers Inc., Brookfield Center, CT, 1987, 45, 146 (Abstract).
12. Erwin, L., in *ANTEC'78 (Ann. Tech. Conf. Soc. Plast. Eng.)*, Washington, DC, ed. New York. Society of Plastics Engineers Inc., Brookfield Center, CT, 1978, 36, 488 (Abstract).
13. Erwin, L., *Polym. Eng. Sci.*, 1978, **18**(7), 572.
14. Ng, K. Y. and Erwin, L., *Polym. Eng. Sci.*, 1981, **21**(4), 212.
15. Rauwendaal, C., in *Polymer Extrusion*, Chapter 7 (Sections 7.4 and 7.7). Hanser Publishers, New York, 1986.
16. Kim, M. H. and White, J. L., in *ANTEC'89 (Ann. Tech. Conf. Soc. Plast. Eng.)* New York, ed. Society of Plastics Engineers Inc., Brookfield Center, CT, 1989, 47, 49 (Abstract).
17. Mack, W. A. and Eise, K., in *Science and Technology of Polymer Processing, Proceedings of the International Conference on Polymer Processing held at MIT*, Cambridge, ed. N. P. Suh and N.-H. Sung. The MIT Press, Cambridge, Massachusetts, 1977, p. 429.
18. Middleman, S., *Fundamentals of Polymer Processing*, Chapter 12 (Sections 12.2-12.4). McGraw-Hill, New York, 1977.
19. Yang, L.-Y., Bigio, D. and Smith, T. G., *J. Appl. Polym. Sci.*, 1995, **58**, 129.
20. Min, K. and White, J. L., *Rubber Chem. Technol.*, 1985, **58**, 1024.
21. Min, K., *Intern. Polym. Process.*, 1987, **1**(4), 179.
22. Cheng, J. J. and Manas-Zloczower, I., *Intern. Polym. Process.*, 1990, **5**(3), 178.
23. Tadmor, Z. and Gogos, C. G., *Principles of Polymer Processing*, Chapter 11 (Section 11.9). John Wiley and Sons, New York, 1979.
24. Bikker, J. A., Smith, R. and Baker, W. E., in *ANTEC '89 (Ann. Tech. Conf. Soc. Plast. Eng.)*, New York, ed. Society of Plastics Engineers Inc., Brookfield Center, CT, 1989, 47, 129 (Abstract).
25. Freakley, P. K. and Wan Idris, W. Y., *Rubber Chem. Technol.*, 1979, **52**, 134.
26. Min, K. and White, J. L., *Rubber Chem. Technol.*, 1987, **60**, 361.
27. Min, K., *Adv. Polym. Technol.*, 1987, **7**(3), 243.
28. White, J. L. and Min, K., *Makromol. Chem., Macromol. Symp.*, 1988, **16**, 19.
29. David, B., Sapir, T., Nir, A. and Tadmor, Z., *Intern. Polym. Process.*, 1990, **5**(3), 155.
30. Tadmor Z., Technical Report. The Japan Steel Works Ltd., 1990, 44, 3.
31. Wong, T. H. and Manas-Zloczower, I., *Intern. Polym. Process.*, 1994, **9**(1), 3.
32. Yamaoka, I. and Kimura, M., *Polymer*, 1993, **34**, 4399.
33. Bailey, F. W., U.S. Patent 4, 386, 190, 1983.
34. Kitchen, A. D. and Sara, F. J., Japanese Examined Patent Publication No. 48-4106, 1973.
35. Freakley, P. K. and Patel, S. R., *Polym. Eng. Sci.*, 1987, **27**(18), 1358.
36. Hu, B. and White, J. L., *Rubber World*, 1993, **208**(4), 17.
37. Blyler, L. L. Jr and Daane, J. H., *Polym. Prep., Am. Chem. Soc., Div. Polym. Chem.*, 1967, **8**(1), 433.
38. Tadmor, Z. and Gogos, C. G., in *Principles of Polymer Processing*, Chapter 10 (Sections 10.2 and 10.3). John Wiley, New York, 1979.
39. Rauwendaal, C., *Mixing in Polymer Processing*, ed. C. Rauwendaal, Chapter 4 (Section 2.1). Marcel Dekker, New York, 1991.
40. Ito, K., *Purasuchikkusu*, 1983, **34**(9), 113.
41. Stevens, M. J., *Extruder Principles and Operation*, Chapter 5 (Section 5.7). Elsevier Applied Science, London, 1985.
42. Fukuoka, T. and Min, K., *Polym. Eng. Sci.*, 1994, **34**(13), 1033.
43. Ito, K., *Purasuchikkusu*, 1984, **35**(2), 99.
44. McKelvey, J. M., *Polymer Processing*. John Wiley, New York, 1962, p. 299.
45. Erwin, L., *Polym. Eng. Sci.*, 1978, **18**(9), 738.
46. Erwin, L., *Polym. Eng. Sci.*, 1978, **18**(13), 1044.
47. Tadmor, Z. and Gogos, C. G., *Principles of Polymer Processing*, Chapter 7 (Section 7.10). John Wiley, New York, 1979.
48. Hobbs, S. Y., *J. Macromol., Sci.-Rev. Macromol. Chem.*, 1980, **C19**(2), 221.
49. Gebizlioglu, O. S., Argon, A. S. and Cohen, R. E., *Polymer*, 1985, **26**, 519.
50. Mihira, K., Osawa, T. and Nakayama, A., *Sen-i Gakkaishi*, 1967, **23**(8), 386.
51. Mihira, K., Osawa, T. and Nakayama, A., *Kolloid-Zeit.*, 1968, **222**, 135.
52. Goldsmith, P. L., *Brit. J. Appl. Phys.*, 1967, **18**, 813.
53. Saltzman, W. M., Pasternak, S. H. and Langer, R., *Chem. Eng. Sci.*, 1987, **42**(8), 1989.
54. Gleinser, W., Maier, D., Schneider, M., Weese, J., Friedrich, Chr. and Honerkamp, J., *J. Appl. Polym. Sci.*, 1994, **53**, 39.
55. Louis, P. and Gokhale, A. M., *Metall. Mater. Trans. A*, 1995, **26A**(7), 1741.
56. Wu, S., *Polymer*, 1985, **26**, 1855.
57. Wasén, J. and Warren, R., *Mater. Sci. Technol.*, 1989, **5**(3), 222.
58. Friedrich, Chr., Gleinser, W., Korat, E., Maier, D. and Weese, J., *J. Rheol.*, 1995, **39**(6), 1411.
59. Hashimoto, T., Nagatoshi, K., Todo, A., Hasegawa, H. and Kawai, H., *Macromolecules*, 1974, **7**(3), 364.
60. Heikens, D. and Barentsen, W., *Polymer*, 1977, **18**, 69.
61. Tokita, N., *Rubber Chem. Technol.*, 1977, **50**, 292.
62. Sundararaj, U., Macosko, C. W., Rolando, R. J. and Chan, H. T., *Polym. Eng. Sci.*, 1992, **32**(24), 1814.
63. Sundararaj, U., Macosko, C. W., Nakayama, A. and Inoue, T., *Polym. Eng. Sci.*, 1995, **35**(1), 100.
64. Favis, B. D., *J. Appl. Polym. Sci.*, 1990, **39**, 285.
65. Narisawa, I., *Seikei-kakou*, 1991, **3**(1), 6.
66. Narisawa, I., Toyoda, S., Kitamura, T. and Inoue, K., *Seikei-kakou*, 1990, **2**(4), 350.
67. Wu, S., *J. Appl. Polym. Sci.*, 1988, **35**, 549.
68. Wu, S., *Polym. Eng. Sci.*, 1990, **30**(13), 753.